ISSN 1063-7761, Journal of Experimental and Theoretical Physics, 2016, Vol. 122, No. 5, pp. 823–831. © Pleiades Publishing, Inc., 2016.
Original Russian Text © A.N. Kozlov, S.A. Zibrov, A.A. Zibrov, V.I. Yudin, A.V. Taichenachev, E.A. Tsygankov, A.S. Zibrov, V.V. Vassiliev, V.L. Velichansky, 2016, published in Zhurnal Eksperimental'noi i Teoreticheskoi Fiziki, 2016, Vol. 149, No. 5, pp. 955–964.

ATOMS, MOLECULES, OPTICS

Structure of Magnetic Resonance in ^{87}Rb Atoms

A. N. Kozlov[a†], S. A. Zibrov[b, h], A. A. Zibrov[c], V. I. Yudin[d, e, h,*], A. V. Taichenachev[d, e, h], V. P. Yakovlev[f], E. A. Tsygankov[f,], A. S. Zibrov[g, b], V. V. Vassiliev[b, h], and V. L. Velichansky[b, f, h]**

[a] *Pushkov Institute of Terrestrial Magnetism, Ionosphere and Radio Wave Propagation, Russian Academy of Sciences, Troitsk, Moscow, 142190 Russia*

[b] *Lebedev Physical Institute, Russian Academy of Sciences, Leninskii pr. 53, Moscow, 119991 Russia*

[c] *University of California, Santa Barbara, Santa Barbara, CA 93106, USA*

[d] *Institute of Laser Physics, Siberian Branch, Russian Academy of Sciences, pr. Lavrent'eva 13/3, Novosibirsk, 630090 Russia*

[e] *Novosibirsk State University, ul. Pirogova 2, Novosibirsk, 630090 Russia*

[f] *National Research Nuclear University MEPhI, Kashirskoe sh. 31, Moscow, 115409 Russia*

[g] *Harvard University, Cambridge, MA 02138, USA*

[h] *Advanced Energy Technologies Ltd., Cheremushkinskii proezd 5 (office 412), Moscow, 117036 Russia*

** e-mail: viyudin@mail.ru*

*** e-mail: selentinthebright@gmail.com*

Received November 17, 2015

Abstract—Magnetic resonance at the $F_g = 1 \leftrightarrows F_e = 1$ transition of the D_1 line in ^{87}Rb has been studied with pumping and detection by linearly polarized radiation and detection at the double frequency of the radiofrequency field. The intervals of allowed values of the static and alternating magnetic fields in which magnetic resonance has a single maximum have been found. The structure appearing beyond these intervals has been explained. It has been shown that the quadratic Zeeman shift is responsible for the three-peak structure of resonance; the radiofrequency shift results in the appearance of additional extrema in resonance, which can be used to determine the relaxation constant Γ_2. The possibility of application in magnetometry has been discussed.

DOI: 10.1134/S1063776116050071

1. INTRODUCTION

Single magnetic resonance in ^{87}Rb atoms, which can be used to measure magnetic fields B, is studied theoretically and experimentally. Resonance is observed in the absorption of linearly polarized laser radiation on the $F_g = 1 \leftrightarrows F_e = 0; 1; 2$ transitions by the detection of a signal at the double frequency of the radiofrequency (RF) field. Magnetic resonance in alkali metal atoms, primarily, in cesium, potassium, and rubidium has been used in magnetometry for more than five decades [1–3]. For first three decades, the frequency of Larmor precession of the angular momentum of atoms was detected in the absorption of the radiation of resonance lamps filled with the same atoms as in a detector cell. As the capabilities of this method have been exhausted, the replacement of resonance lamps by diode lasers, whose many characteristics are better than those of lamps, became more attractive. The first such work [4], on one hand, demonstrated that the application of diode lasers in magnetometers is promising and, on the other hand, revealed their disadvantages. An increase in the reliability of the single-mode generation regime and reproducibility of the spectral characteristics of diode lasers stimulated investigations of new variants of magnetometers [5–8].

Potassium, rubidium, and cesium atoms are similar in certain characteristics: their resonant wavelengths are in the spectral range in which diode lasers operate and magnetic moments are close in the order of magnitude. However, there are differences important for magnetometry (see table), primarily in the quadratic Zeeman shift and working temperature (these data are presented under the assumption of identical dimensions of resonance cells).

Since the quadratic Zeeman shift for potassium is large, transitions between different Zeeman sublevels in the Earth's magnetic field are resolved and measurements can be performed on a single line. Owing to this circumstance, the sensitivity of potassium magnetometers at the measurement of the Earth's fields is significantly higher than that of cesium or rubidium magnetometers. In the latter magnetometers, several

† Deceased.

Table 1

	^{39}K	^{87}Rb	^{133}Cs
Quadratic shift, Hz/G^2	1063	71.8	13.3
Working temperature, °C	70	50	40

resonances are superimposed (no less than two for ^{87}Rb, four for ^{85}Rb, and six for Cs). This leads not only to the broadening of the resonance and to lower sensitivity, but also to additional errors because of the asymmetry of the line and its dependence on the orientation of the detector with respect to the measured field. Nevertheless, cesium magnetometers are the most widespread magnetometers with optical pumping because cesium-filled cells have lower working temperature and lower energy consumption. A narrow symmetric line was observed in Cs atoms at the detection of magnetic resonance at the double frequency for the RF field [9, 10] but for magnetic fields much weaker than the terrestrial magnetic field when the quadratic Zeeman shift can be neglected as compared to the linewidth. In this work, we study the situation where the advantages of a single line and a comparatively low working temperature are joined in a ^{87}Rb-based magnetometer for the Earth's fields.

The idea of the detection of a single resonance is as follows. Two one-photon transitions in the RF field are possible between adjacent magnetic sublevels $m_F = -1, 0, 1$ of the ground level with $F_g = 1$. Consequently, at pumping by circularly polarized optical radiation and probing by the RF field, two close resonances are observed. However, for excitation by linearly polarized radiation, only one resonance in a signal oscillating at the double frequency of the RF field can be observed. This resonance appears at the two-photon transition between the extreme sublevels $m_F = -1$ and 1; the interval between them is independent of the quadratic Zeeman shift. The lineshape of magnetic resonance under these conditions is studied theoretically and experimentally in this work.

2. EXPERIMENT

The results presented in this section confirm the possibility of the detection of a single resonance in the proposed scheme and determine the ranges of measured magnetic fields and amplitudes of the probe alternating RF field in which the symmetry of the amplitude, as well as the presence of only one maximum, is conserved. Changes in the lineshape observed beyond the indicated ranges are described. The theory presented in the next section adequately describes the experimentally observed variations of the shape. For convenience of comparison, some experimental results will be reported in the next section.

The layout of the experimental setup is shown in Fig. 1. A diode laser with an external cavity whose design allowed the smooth continuous variation of the frequency within the D_1 line of ^{87}Rb [11] was used as a source of monochromatic radiation resonant to the $F_g = 1 \leftrightarrows F_e = 1$ transition. A fraction of laser radiation tuned to the center of the Doppler line was guided to the frequency stabilization system based on the dichroic atomic vapor laser lock (DAVLL [12]). A cylindrical glass cell (18 mm in length and diameter) with an antirelaxation coating of walls was heated to 47°C, ensuring the density of rubidium vapor 8×10^{10} cm^{-3}. The power of laser radiation directed to the cell was 30 μW at a beam diameter of 3 mm.

The magnetic screen consisting of three μ-metal layers isolated the cell from an inhomogeneous magnetic field. An integrally compensated solenoid [13] placed in the magnetic shield produced a uniform magnetic field **B** collinear with the wavevector **k**. A pair of coils, which were fed by an Agilent 81150a signal generator, produced a harmonic alternating field $\mathbf{B}_{rf}$ orthogonal to **B**. Laser radiation that passed through the cell was detected by a Thorlabs PDA8A photodetector and was analyzed with the use of an

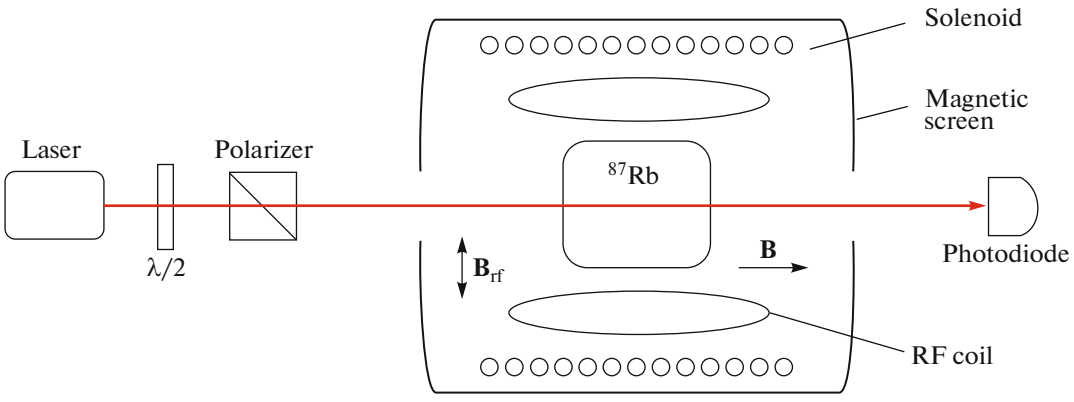

Fig. 1. (Color online) Layout of the experimental setup.

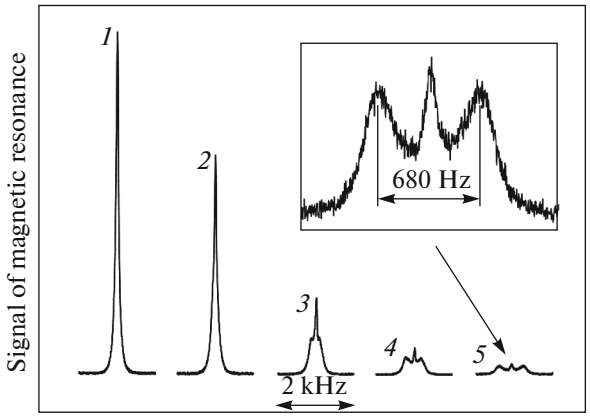

Fig. 2. Evolution of the shape and amplitude of magnetic resonance at the second harmonic of the RF field with the variation of the static magnetic field: (*1*) 0.22, (*2*) 0.87, (*3*) 1.31, (*4*) 1.74, and (*5*) 2.18 G.

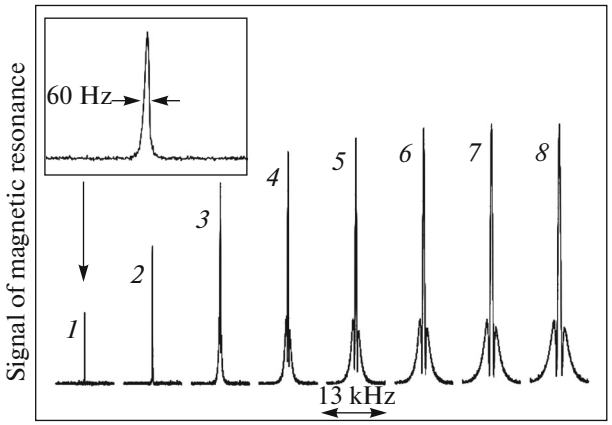

Fig. 3. Evolution of the signal of magnetic resonance at the second harmonic in the magnetic field $B = 0.22$ G with the variation of the amplitude of the RF field from (*1*) 1.5×10^{-5} G. Lines *2*–*8* correspond to the amplitudes larger by factors of 2, 10, 20, 30, 40, 50, and 60, respectively.

Agilent E4405B spectrum analyzer, which was used as a narrowband filter and operated in the absence of scanning.

It was found that the orthogonality of the polarization of laser radiation to the static magnetic field ensured the maximum signal of absorption modulation at the double frequency of the RF field. To this end, at the switched-off field of the solenoid **B**, an additional pair of coils produced a static field **B'** orthogonal to $\mathbf{B}_{rf}$ and **k**. Under these conditions, the rotation of the plane of polarization of laser radiation allowed recording the dependence of the signal level on the angle θ between **B'** and **E**.

Figure 2 shows the dependence of the signal of magnetic resonance, i.e., the transmittance of the cell at the double frequency on the frequency of the RF field, for various static magnetic fields. It is seen that resonance has a symmetric shape and a single maximum in the interval of static magnetic fields of up to 1 G. With an increase in the static magnetic field, the amplitude of the signal decreases and two additional lateral maxima appear without the violation of the symmetry of the line. The measurements showed that the distances of these maxima from the central peak almost coincide with the quadratic Zeeman shift.

The effect of the amplitude of the RF field on the signal of the second harmonic of magnetic resonance was studied in a static magnetic field of 0.22 G. In this case, as the amplitude of the RF field increases, two lateral maxima symmetric with respect to the central resonance also appeared in the signal of absorption modulation (Fig. 3). The minor asymmetry of the lateral maxima in amplitude is due to a high scanning rate.

We also study the effect of the amplitude of the RF field on the signal of the first harmonic of magnetic resonance. The signal at the first harmonic in the case where $\mathbf{E} \perp \mathbf{B}$ is below the noise level. For this reason, to detect this signal, the solenoid was rotated by an angle of 0.01 rad at the conservation of the orthogonality of **B** to $\mathbf{B}_{rf}$. The signal of magnetic resonance obtained at $B = 0.22$ G and $B_{rf} = 6 \times 10^{-4}$ G is shown in Fig. 4. It is seen that the structure of the signal of magnetic resonance at the frequency of the RF field is significantly more complex (the central region contains five extrema) than that at the double frequency.

3. THEORY

3.1. Formulation of the Problem

The detector of the quantum magnetometer with laser pumping is a cell that was filled with alkali-metal

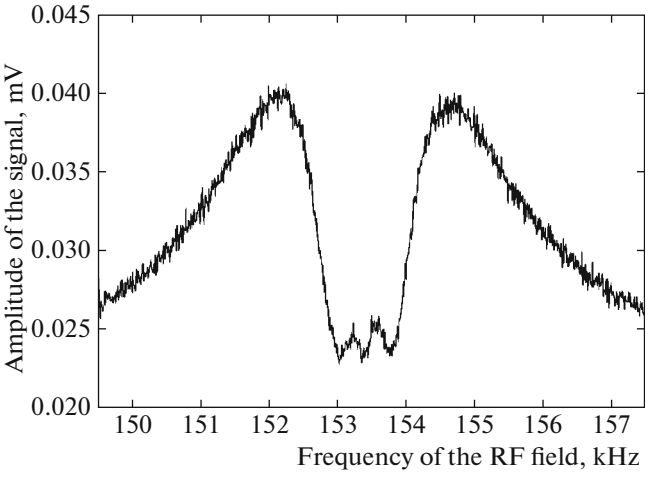

Fig. 4. Signal of magnetic resonance at the first harmonic in magnetic fields $B = 0.22$ G and $B_{rf} = 6 \times 10^{-4}$ G.

atoms with the ground state degenerate in projections of the angular momentum and was in the static magnetic field **B**, which was measured. The system was subjected both to a linearly polarized monochromatic laser wave $\mathbf{E}\cos(\mathbf{k}\cdot\mathbf{r} - \omega_l t)$, which has a small detuning $\Delta = \omega_l - \omega_0$ from the frequency ω_0 of the working optical transition for a free atom at rest, and to the RF magnetic field $\mathbf{B}_{\rm rf}\cos\omega_{\rm rf}t$.

The static magnetic field **B**, whose direction is taken as the z quantization axis, is responsible for the linear Zeeman splitting with the interval $\omega_B = g\mu B/\hbar$. The RF field $\mathbf{B}_{\rm rf}$ oriented along the x axis, has the small detuning $\delta = \omega_{\rm rf} - \omega_B$ from the frequency of Zeeman splitting and is responsible for the resonance mixing of the neighboring sublevels of the ground state. Finally, for generality, we assume that the angle between the electric field $\mathbf{E} = \{\mathbf{E}_\perp, E_z\}$ and z axis is θ; hence, $E_z = E\cos\theta$ and $E_\perp = E\sin\theta$.

This configuration of fields ensures magnetic resonance, which is detected in the dependence of the absorption coefficient of the laser wave on the frequency $\omega_{\rm rf}$. The characteristic feature of this situation is that the absorption coefficient includes not only a constant term but also contributions oscillating at frequencies multiple of $\omega_{\rm rf}$. Such harmonics appear in the absorption coefficient because of the effect of the RF field, which induces coherence in the sublevels of the ground state of atoms that periodically depends on time at the indicated frequencies.

The angular momentum of the ground state of the most widespread isotopes of alkali metals is an integer; consequently, the simplest structure of magnetic resonance can be implemented for the angular momentum $F_{\rm g} = 1$. For this reason, for the theoretical description of the structure of the absorption coefficient of the laser wave, we consider below the $|g, F_{\rm g} = 1\rangle \leftrightarrows |e, F_{\rm e} = 1\rangle$ optical atomic transition, which occurs, e.g., for one of four hyperfine components of the D_1 line in ^{87}Rb and was experimentally studied.

In addition to the above quantities (ω_B and $\omega_{\rm rf}$, as well as small detunings Δ and δ), the problem includes several additional frequencies such as the constant γ of the spontaneous relaxation of the excited state; Rabi frequencies of various induced electric dipole $|g, 1, m_{\rm g}\rangle \leftrightarrows |e, 1, m_{\rm e}\rangle$ transitions, which are determined by the longitudinal (E_z) or transverse ($E_\perp$) components (with respect to static magnetic field B) of the laser field with the corresponding Clebsch–Gordan coefficients and are proportional to $\Omega = dE/2\hbar$; and the Rabi frequency $\Omega_{\rm rf} = g\mu B_{\rm rf}/2\hbar$ of magnetic dipole transitions between the neighboring sublevels of the ground state.

The case of sufficiently weak fields whose characteristic frequencies satisfy the hierarchy

$$\Omega, \Omega_{\rm rf} \ll \omega_B \ll \gamma. \qquad (1)$$

is of the most interest for physical applications. It is noteworthy that the effect of the static and RF magnetic fields on the excited state can be neglected in this situation and the equations for the atomic density matrix are significantly simplified.

3.2. Density Matrix of the Ground State and the Absorption Coefficient

According to Eq. (1), alternating fields (optical and RF) are weak; therefore, the excited state can be adiabatically excluded from the equations for the density matrix and the resonance approximation in the interaction with the RF magnetic field can be used in the resulting equations for the density matrix $\rho^{gg}_{\rm mm'}$ of the ground state. In this case, it is convenient to separate in the off-diagonal elements the phase factors "rapidly" oscillating at frequencies multiple of $\omega_{\rm rf}$, namely,

$$\rho^{gg}_{10}(t) = \rho_{10}\exp(-i\omega_{\rm rf}t),$$

$$\rho^{gg}_{0-1}(t) = \rho_{0-1}\exp(-i\omega_{\rm rf}t),$$

$$\rho^{gg}_{1-1}(t) = \rho_{1-1}\exp(-2i\omega_{\rm rf}t),$$

and to omit the antiresonance terms.

This procedure, which is equivalent, as is known, to the rotating wave approximation, eliminates the time dependence of the coefficients of equations. If the energy of magnetic sublevels increases with m, resonance transitions correspond to the σ_+ polarization (with respect to the z axis) of the alternating magnetic field. The direction of the x axis for the rotating field becomes insignificant and can be chosen along the vector $\mathbf{E}_\perp$.

Relaxation processes in the system such as collisions with a buffer gas or a wall having the antirelaxation coating ensure the steady-state behavior of the atomic ensemble and they can be included phenomenologically by means of three constants Γ, Γ_1, and Γ_2. They describe the relaxation rate of populations (Γ) and coherence relaxation rates between neighboring (Γ_1) and extreme (Γ_2) sublevels. Since relaxation constants determine the width of radio-optical resonance, they should be sufficiently small for physical applications so that $\Gamma, \Gamma_1, \Gamma_2 \ll \omega_B$. At the same time, it can be assumed that in a weak laser field, the condition $\Omega^2/\gamma \ll \Gamma, \Gamma_1, \Gamma_2$ is satisfied; under this condition, the terms $\Omega^2/(\Delta + i\gamma/2)$, which describe complex light shifts, can be neglected.

It is reasonable to represent the diagonal elements in the steady-state equations in the form $\rho^{gg}_{\rm mm} = 1/3 + \rho_{\rm mm}$, i.e., to separate the equilibrium populations so that $\mathrm{Tr}\hat{\rho} = 0$. As a result, we arrive at the system of equations

$$\Gamma\rho_{11} = i\Omega_{\rm rf}(\rho_{10} - \rho_{01}) + (\gamma/4)S_p(\theta), \qquad (2a)$$

$$(\delta_- + i\Gamma_1)\rho_{10} + \Omega_{\rm rf}(2\rho_{11} + \rho_{-1-1} + \rho_{1-1}) = 0, \qquad (2b)$$

$$(\delta_+ + i\Gamma_1)\rho_{0-1} - \Omega_{rf}(\rho_{11} + 2\rho_{-1-1} + \rho_{1-1}) = 0, \quad (2c)$$

$$(2\delta + i\Gamma_2)\rho_{1-1} + \Omega_{rf}(\rho_{10} - \rho_{0-1}) = 0. \quad (2d)$$

Here, $S_p(\theta) = S(1/3 - \cos^2\theta)$, where $S = \Omega^2/(\Delta^2(\mathbf{v}) + \gamma^2/4)$ is the saturation parameter for the laser field with detuning $\Delta(\mathbf{v}) = \Delta - \mathbf{k}\cdot\mathbf{v}$, which includes the Doppler shift; for generality, RF detunings $\delta_\mp = \delta \mp \omega_{B^2}$ include the quadratic Zeeman shift, which, as is known, results in the same positive shifts of the sublevels with $m = \pm 1$ by $\hbar\omega_{B^2}$. It is taken into account in the equations that $\rho_{00} = -\rho_{11} - \rho_{-1-1}$. In this case, the equation for ρ_{-1-1}, which is not presented in an explicit form, is obtained from Eq. (2a) by the replacement of the subscritpt 1 by -1.

We point to some features of the system of equations (2a)–(2d). The interaction with a weak laser wave appears in Eq. (2a) for the population ρ_{11} and in the equation for ρ_{-1-1} only in the form of the inhomogeneous term $(\gamma/4)\,S_p(\theta)$. This quantity is the optical pumping rate of the extreme sublevels, which violates the uniform population of the sublevels of the ground state. The angular dependence in $S_p(\theta)$ is due to the longitudinal and transverse components of the electric field, which induce transitions without and with a change in the projection of the angular momentum, respectively. At angles satisfying the condition $\cos^2\theta > 1/3$, "vertical" ($\Delta m = 0$) transitions prevail; since such transitions from the $m = 0$ state are forbidden, the population of this state increases so that $S_p(\theta) < 0$. On the contrary, transitions with a change in the projection of the angular momentum prevail if $\cos^2\theta < 1/3$; as is known, these transitions result in the pumping of extreme sublevels, i.e., $S_p(\theta) > 0$.

We emphasize that optical pumping is inevitably necessary. Indeed, system (2) at $S_p(\theta) = 0$ has only the trivial solution $\hat\rho = 0$, so that the density matrix is $\hat\rho^{gg} = 1/3$ and magnetic resonance is absent.

Although the system of equations (2) is obtained for the $|g, F_g = 1\rangle \leftrightarrows |e, F_e = 1\rangle$ transition, under the accepted approximations, it holds the form for transitions with other angular momenta of the excited state $F_e = 0, 2$. Only the expression for the source $S_p(\theta)$ changes.

The absorption coefficient of the laser wave is proportional to the population $\mathrm{Tr}\hat\rho^{ee}$ of the excited state, which is in turn expressed in terms of the elements of the density matrix of the ground state, which satisfy Eqs. (2a)–(2d). The absorption signal includes not only the constant term but also two contributions of interest, which oscillate at the frequencies ω_{rf} and $2\omega_{rf}$ and are described by the expressions

$$\kappa_1(t) \sim \langle S_1(\theta)\cdot \mathrm{Re}[(\rho_{10} - \rho_{0-1})\exp(-i\omega_{rf}t)]\rangle, \quad (3a)$$

$$\kappa_2(t) \sim \langle S_2(\theta)\cdot \mathrm{Re}[\rho_{1-1}\exp(-2i\omega_{rf}t)]\rangle. \quad (3b)$$

Here, the angular brackets mean averaging with the velocity distribution function $S_1(\theta) = S\sin 2\theta$ and $S_2(\theta) = S\sin^2\theta$, where S is the previously introduced saturation parameter.

The first harmonic $\kappa_1(t)$ is related to the populations ρ_{11}^{ee} and ρ_{-1-1}^{ee} of the extreme sublevels of the excited state which are related to coherences induced by the RF field between the neighboring sublevels of the ground state. The related contributions are determined by the product of two field amplitudes—with and without a change in the projection of the angular momentum, i.e., $\kappa_1(t) \sim E_\perp E_z \sim E^2\sin 2\theta$.

The second harmonic $\kappa_2(t)$ is related to the population ρ_{00}^{ee}, which includes coherence induced by the RF field between the extreme sublevels of the ground state, as occurs in the standard Λ-configuration of transitions. For this reason, the indicated contribution is determined by the product of two probability amplitudes of transitions with a change in the projection of the angular momentum, which are in turn proportional to the transverse component of the electric field so that $\kappa_2(t) \sim E_\perp^2 \sim E^2\sin^2\theta$.

According to the structure of Eqs. (2a)–(2d), all elements of the density matrix of the ground state are proportional to $S_p(\theta)$, which appears in the solution as a common factor. Consequently, harmonics (3a) and (3b) of the absorption coefficient are proportional to S^2; i.e., the effect is quadratic in the intensity of a weak laser field. This nonlinearity is quite obvious because harmonics appear only when the same field is responsible for the optical pump of the ground state.

The dependence of the velocity of atoms appears in the saturation parameter S only in the form of the Doppler shift. Consequently, averaging over velocities results in the appearance of the common scaling factor

$$\langle S^2\rangle \approx \sqrt{\pi}\left(\frac{2\Omega^2}{\gamma^2}\right)^2 \frac{\gamma}{kv_T},$$

in κ_1 and κ_2, where v_T is the characteristic thermal velocity, which will be omitted below for brevity.

3.3. Effect of the RF Shift on the Structure of Harmonics of Absorption Resonance

The resonance structure of $\kappa_1(t)$ and $\kappa_2(t)$ was recorded as a function of δ at the variation of the frequency of the RF field near the Zeeman frequency ω_B. The characteristic width is determined by the relaxation constants Γ_1 and Γ_2, i.e., $|\delta| \sim \Gamma_{1,2}$. If $\omega_{B^2} \ll \Gamma_{1,2}$, the quadratic Zeeman effect can be neglected setting $\delta_- = \delta_+ = \delta$ in Eqs. (2b) and (2c). In this case, there is a certain symmetry between adjacent transitions and, as a result, the solution of the equations satisfies the relations $\rho_{-1-1} = \rho_{11}$ and $\rho_{0-1} = -\rho_{10}$.

In view of these relations, it follows from Eq. (2b) that the coefficient of ρ_{10} includes the additional term $-\Omega_{rf}^2/(\delta + i\Gamma_2/2)$, which is the complex RF shift owing to the two-photon resonance transition between the sublevels with $m = \pm 1$ through an intermediate state with $m = 0$. As a result, the detuning of resonance and the relaxation constant are renormalized:

$$\delta + i\Gamma_1 \to \tilde{\delta} + i\tilde{\Gamma}_1,$$

where

$$\tilde{\delta} = \delta\left(1 - \frac{\Omega_{rf}^2}{\delta^2 + \Gamma_2^2/4}\right), \quad (4a)$$

$$\tilde{\Gamma}_1 = \Gamma_1\left(1 + \frac{1}{2}\frac{\Omega_{rf}^2}{\delta^2 + \Gamma_2^2/4}\right). \quad (4b)$$

An important feature of the effective detuning $\tilde{\delta}$ as a function of $\delta = \omega_{rf} - \omega_B$ is that it vanishes not only at the point $\delta = 0$, but also at the points $\pm\delta_0$, where it has two real-valued roots, in the case $\Omega_{rf} > \Gamma_2/2$, where

$$\delta_0 = \sqrt{\Omega_{rf}^2 - \Gamma_2^2/4}. \quad (5)$$

Such a behavior of the function $\tilde{\delta}(\delta)$ significantly affects the structure of the harmonics of the absorption resonance.

Let $\Gamma_1 = \Gamma_2 = \Gamma$ for simplicity. Then, harmonics (3a) and (3b) of the absorption coefficient have the form (the common factor $\langle S^2\rangle$ is omitted for brevity)

$$\kappa_{1,2}(t) \sim F_{1,2}(\theta)\,\mathrm{Re}[\mathscr{A}_{1,2}\exp(-i\omega_{1,2}t)]. \quad (6)$$

Here,

$$F_1(\theta) = (1/3 - \cos^2\theta)\sin 2\theta,$$

$$F_2(\theta) = (1/3 - \cos^2\theta)\sin^2\theta,$$

$\omega_1 \equiv \omega_{rf}$, $\omega_2 \equiv 2\omega_{rf}$, and the complex amplitudes $\mathscr{A}_{1,2}$ are given by the expressions

$$\mathscr{A}_1 = -\Omega_{rf}\frac{\tilde{\delta} - i\tilde{\Gamma}}{\tilde{\delta}^2 + \tilde{\Gamma}(\tilde{\Gamma} + 6\Omega_{rf}^2/\Gamma)}, \quad (7a)$$

$$\mathscr{A}_2 = \Omega_{rf}^2\frac{(\delta - i\Gamma/2)(\delta - i\Gamma) - \Omega_{rf}^2}{(\delta^2 + 2\Omega_{rf}^2 + \Gamma^2)(\delta^2 + 2\Omega_{rf}^2 + \Gamma^2/4)}. \quad (7b)$$

The dependence of the amplitudes of the harmonics on the orientation of the polarization **E** of the laser wave with respect to the direction of the static magnetic field **B** is determined by the functions $|F_1(\theta)|$ and $|F_2(\theta)|$. In the interval $0 \leqslant \theta \leqslant \pi/2$, each of these functions vanishes at the point where $\cos^2\theta = 1/3$ and has local maxima to the left and right. The function $|F_1(\theta)|$ is maximal at the angle $\theta_m \approx 0.148\pi$ (25.52°), where the longitudinal component of the electric field is approximately twice as large as the transverse component. The function $|F_2(\theta)|$ is maximal at $\theta = \pi/2$, where **E** and **B** are orthogonal to each other; this is obvious because transitions with a change in the projection of the angular momentum, which create the maximum coherence of ρ_{1-1}, are induced in this case.

The dependence of the signals of the first and second harmonics of magnetic resonance on the detuning δ is determined by the quantities $|\mathscr{A}_{1,2}|$. According to Eqs. (7a) and (7b), they depend only on δ^2 and are specified by the expressions

$$|\mathscr{A}_{1,2}(\delta^2)| = \frac{\sqrt{Q_{3,2}(\delta^2)}}{P_2(\delta^2)},$$

where Q_3 is the third-order polynomial and Q_2 and P_2 are the second-order polynomials. The last polynomial is the denominator in Eq. (7b) (and, in view of Eqs. (4), the denominator in Eq. (7a)) and is a monotonically increasing function because all its coefficients are positive. The coefficients of the polynomials Q_3 and Q_2 are generally not sign-definite; consequently, the behavior of these functions can be nonmonotonic. It is obvious that the behavior of the function $\mathscr{A}_1(\delta^2)$, which includes the third-order polynomial Q_3, is more complex than the behavior of the function $\mathscr{A}_2(\delta^2)$, which depends on the second-order polynomial Q_2.

In the case of a weak RF field, where $\Omega_{rf} \ll \Gamma$, these functions have the form

$$|\mathscr{A}_1| = \frac{\Omega_{rf}}{\sqrt{\delta^2 + \Gamma^2}}, \quad (8a)$$

$$|\mathscr{A}_2| = \frac{\Omega_{rf}^2}{\sqrt{(\delta^2 + \Gamma^2)(\delta^2 + \Gamma^2/4)}} \quad (8b)$$

and decrease monotonically with an increase in the detuning δ.

With an increase in the RF field in the region $\Omega_{rf} \geq \Gamma$, the RF shift plays a significant role and the shape of resonances becomes more complex.

According to Eq. (7a), which gives the explicit dependence of the amplitude $\mathscr{A}_1$ on the effective detuning $\tilde{\delta}$, the function $|\mathscr{A}_1(\delta^2)|$ at $\Omega_{rf} > \Gamma/2$ has local minima at the points where $\tilde{\delta} = 0$, i.e., at $\delta = 0$ and $|\delta| = \delta_0$. At these points, the function $\mathscr{A}_1$ is pure imaginary; therefore, $\kappa_1(t) \sim \sin\omega_{rf}t$. Local maxima obviously exist in the ranges $0 < |\delta| < \delta_0$. It is noteworthy that the function $|\mathscr{A}_1(\delta^2)|$ has a maximum or a minimum at the point $\delta = 0$ if $\Omega_{rf} < 0.19\Gamma$ or $\Omega_{rf} > 0.19\Gamma$, respectively. The thin solid line in Fig. 5 demonstrates such a nontrivial behavior of $|\mathscr{A}_1|$ and is in good agreement with the experimental curve shown in Fig. 4.

We now discuss the manifestation of the RF shift in the structure of the second harmonic of magnetic resonance. With an increase in Ω_{rf}, the monotonic decrease in the function $|\mathscr{A}_2(\delta^2)|$ according to Eq. (8)

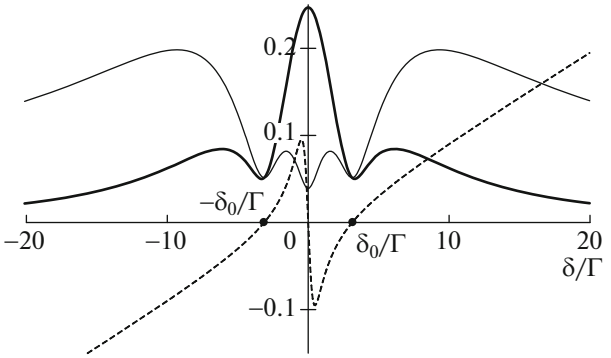

Fig. 5. Resonance structure of the amplitudes of the (thin line) first ($|\mathcal{A}_1|$) and (thick line) second ($|\mathcal{A}_2|$ harmonics of magnetic resonance at the parameter $(\Omega_{rf}/\Gamma)^2 = 10$. The dashed line is the function $0.01\tilde{\delta}/\Gamma$.

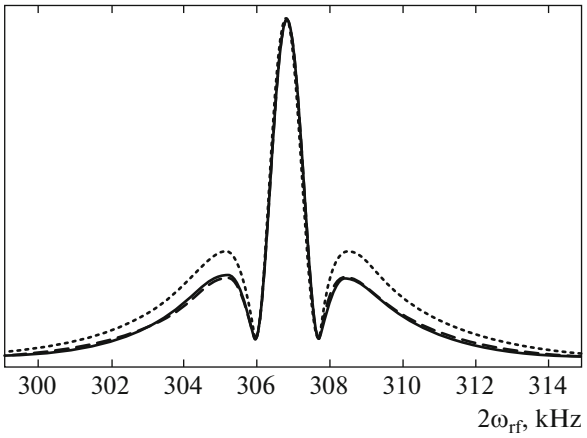

Fig. 6. Experimental curve *6* from Fig. 3 after hundredfold averaging. The dotted line is the theoretical curve at $\Gamma = \Gamma_1 = \Gamma_2 \approx 48$ Hz. The dashed line is the theoretical curve at $\Gamma \approx 74$ Hz, $\Gamma_1 \approx 71$ Hz, and $\Gamma_2 \approx 47$ Hz. All data were obtained with the parameter $\Omega_{rf} \approx 427$ Hz. The horizontal axis shows the double frequency of the RF field.

is violated and inflection points appear on the slopes of the curve when $\Omega_{rf} = 2\Gamma$. Local minima and maxima appear on these slopes at larger parameters Ω_{rf}/Γ. In other words, a "fold catastrophe" occurs for the inverse function δ^2 ($|\mathcal{A}_2|$). Such a behavior of $|\mathcal{A}_2(\delta^2)|$ becomes particularly pronounced in the region $\Omega_{rf} \gg \Gamma$, where the shape of resonance is described by the simpler expression

$$|A_2(\delta^2)| = \Omega_{rf}^2 \frac{\sqrt{(\delta^2 - \Omega_{rf}^2)^2 + (3\Gamma\Omega_{rf}/2)^2}}{(\delta^2 + 2\Omega_{rf}^2)^2}. \qquad (9)$$

This function has a maximum ($\approx 1/4$) at the point $\delta = 0$. In addition, this function has a local minimum ($\approx \Gamma/6\Omega_{rf}$) at the point $|\delta| \approx \delta_0 \approx \Omega_{rf}$ and a local maximum ($\approx 1/12$) at the point $|\delta| \approx 2\Omega_{rf}$. It is noteworthy that the local minimum is near the point $\tilde{\delta} = 0$, so that the width of the central peak in the strong RF field is about Ω_{rf}. These features and characteristic scales are seen on the thick solid line in Fig. 5.

For clear comparison, Fig. 5 shows the function $\tilde{\delta}(\delta)/\Gamma$ in a reduced scale, which demonstrates that the minima of the function $|\mathcal{A}_1(\tilde{\delta})|$ are at the points where $\tilde{\delta} = 0$, and the minima of the function $|\mathcal{A}_2(\tilde{\delta})|$ are near these points, as was discussed above.

Expressions (7a) and (7b) were obtained under the simplifying assumption that the relaxation constants in Eq. (2) are equal to each other. The positions of minima of the functions $|\mathcal{A}_1(\tilde{\delta})|$ and $|\mathcal{A}_2(\tilde{\delta})|$ are determined by the quantity δ_0 given by Eq. (5), which includes only the constant Γ_2. Then, comparison with experimental curve *8* in Fig. 3 gives $\Gamma_2 \approx 48$ Hz. The validity of this estimate is confirmed by a more detailed theoretical calculation without the assumption of the equality of the constants. The corresponding lengthy analytical expressions are not presented here and the results are shown in Fig. 6 in comparison with the experiment. Such a comparison with the more detailed theoretical calculation makes it possible to estimate not only the constant Γ_2, but also the other two constants Γ and Γ_1. The resulting constant Γ_2, which describes the relaxation of coherence on the extreme sublevels, is smaller than the constant Γ_1 of relaxation of coherences on the neighboring sublevels by a factor of 1.5. This is in agreement with the general statement on a decrease in the width of resonances with an increase in multiplicity [14, 15].

3.4. Influence of the Quadratic Zeeman Effect on the Structure of the Second Harmonic of Absorption Resonance

Owing to the quadratic Zeeman effect, the frequency intervals between the neighboring sublevels of the ground state become unequal. One interval decreases by the value ω_{B^2} and the detuning is δ_+ and the other interval increases, giving the detuning δ_-. The interval between the extreme sublevels does not change and the detuning is equal to 2δ. This effect can play a significant role if $\omega_{B^2} \geqslant \Gamma, \Gamma_1, \Gamma_2$. In this case, the frequency of the RF field at variation passes through various resonances associated with the detunings $\delta_\pm$ and 2δ.

As is known, only two resonances near $\delta = \pm\omega_{B^2}$ are superimposed in the amplitude of the first harmonic of the absorption coefficient. It is more interesting to consider the influence of the quadratic Zeeman effect on the structure of the amplitude of the second harmonic to which all three resonances contribute.

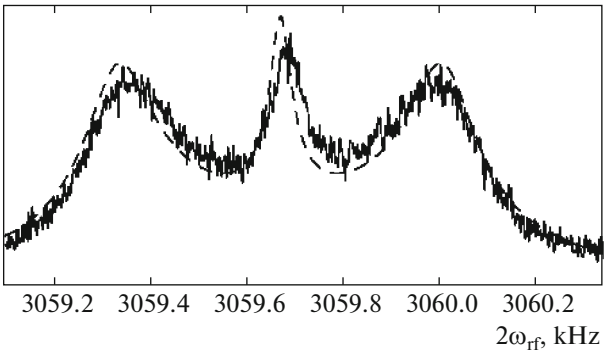

Fig. 7. Experimental curve *5* from Fig. 2. The dashed line is the theoretical curve for $|\mathcal{A}_2|$ at $\Gamma_1 \approx 71$ Hz, $\Gamma_2 \approx 46$ Hz, and $\omega_{B^2} \approx 340$ Hz. The horizontal axis shows the double frequency of the RF field.

In the case of a weak RF field where $\Omega_{rf} \ll \Gamma, \Gamma_1, \Gamma_2$, the solution of Eqs. (2a)–(2d) gives the following expression for the amplitude of the second harmonic:

$$\mathcal{A}_2 = \frac{\Omega_{rf}^2/2}{\delta + i\Gamma_2/2}\left(\frac{1}{\delta_+ + i\Gamma_1} + \frac{1}{\delta_- + i\Gamma_1}\right), \qquad (10)$$

where the individual relaxation constants for one-photon (Γ_1) and two-photon (Γ_2) transitions are retained for clarity. The terms in the parentheses are responsible for resonance contributions at the shifted frequencies $\delta = \pm\omega_{B^2}$. Both these resonances expectedly have the width Γ_1. The factor in front of the parenthesis corresponds to the two-photon resonance $\delta = 0$ between the extreme sublevels. The width of this resonance is determined by the constant Γ_2. For completeness, we note that the function $|\mathcal{A}_2|$ is an even function of δ.

According to Eq. (10), the central resonance is absent in the case $\Gamma_1 = \Gamma_2/2$ (taking into account the fact that $\delta_+ + \delta_- = 2\delta$). This means that the function $|\mathcal{A}_2(\delta^2)|$ can have either a peak ($\Gamma_1 > \Gamma_2/2$) or a dip ($\Gamma_2/2 > \Gamma_1$) near the point $\delta = 0$, depending on the relation between the relaxation constants Γ_1 and Γ_2.

This property is clearly manifested when $\omega_{B^2} \gg \Gamma_1, \Gamma_2$. Then, in the vicinity of $|\delta| \lesssim \Gamma_{1,2}$, we have

$$|\mathcal{A}_2| \approx \left(\frac{\Omega_{rf}}{\omega_{B^2}}\right)^2 \sqrt{\frac{\delta^2 + \Gamma_1^2}{\delta^2 + \Gamma_2^2/4}}. \qquad (11)$$

Experimental curve *5* in Fig. 2 has a peak at the point $\delta = 0$; consequently, $\Gamma_1 > \Gamma_2/2$.

Formula (11), in particular, explains a rapid decrease ($|\mathcal{A}_2| \sim B^{-4}$) in the central peak with an increase in the magnetic field (Fig. 2). The heights of the lateral peaks at the points $|\delta| = \omega_{B^2}$ contain an additional coefficient ω_{B^2}/Γ_1 as compared to Eq. (11) and, thereby, decrease as B^{-2}.

The theoretical results are shown in Fig. 7 in comparison with the experimentally determined three-peak structure where the central and two lateral maxima are resolved. The experimental curve is well approximated by theoretical expression (10) for $|\mathcal{A}_2|$ at the corresponding choice of the relaxation constants Γ_1 and Γ_2.

It is remarkable that estimates of both relaxation constants Γ_1 and Γ_2 coincide quite accurately for noticeably different conditions. Indeed, the results presented in Fig. 6 were obtained for the static magnetic field much weaker than that in Fig. 7, whereas the relation for the RF field is opposite.

4. CONCLUSIONS

The possibility of the observation of single magnetic resonance in ^{87}Rb at the recording of the absorption signal of linearly polarized radiation at the double radio frequency of modulation of the magnetic field has been confirmed experimentally and theoretically. The theory adequately describes the experimental results: the maximum of the signal at the second harmonic for the polarization of laser radiation perpendicular to the static magnetic field (Eq. (3b)); a complex contour of the line in a quite strong static magnetic field because of the quadratic Zeeman shift (Fig. 2, Eq. (10)); and the appearance of additional extrema in the magnetic resonance contour under the variation of the amplitude of the RF field (Fig. 3, Eq. (7b)). The structure of magnetic resonance, which appears because of the RF shift, makes it possible to estimate the relaxation constants.

It is noteworthy that nature "favors" the application of the considered type of magnetic resonance for measuring the Earth's magnetic field because (a) the complication of the structure of the line is observed in fields higher than the Earth's magnetic field and lateral resonances even in such fields do not affect the position of the central peak and do not violate its symmetry and (b) the much lower amplitude of the alternating magnetic field than those at which additional extrema appear is sufficient for the detection of magnetic resonance with the necessary signal-to-noise ratio.

The use of a narrow symmetric line in ^{87}Rb atoms will allow a significant reduction of the orientational shift and an increase in the sensitivity to variations of the Earth's magnetic field at least by an order of magnitude as compared to cesium magnetometers.

ACKNOWLEDGMENTS

We are grateful to A.K. Vershovskii and A.S. Pazgalev for stimulating discussion. The work of

S.A. Zibrov was supported by the Educational–Scientific Complex, Lebedev Physical Institute. The work of A.V. Taichenachev and V.I. Yudin was supported by the Ministry of Education and Science of the Russian Federation (state assignment no. 2014/139, project no. 825), by the Russian Foundation for Basic Research (project nos. 15-02-08377, 14-02-00712, 14-02-00806, and 14-02-00939), and by the Council of the President of the Russian Federation for Support of Young Scientists and Leading Scientific Schools (project no. NSh-4096.2014.2).

REFERENCES

1. N. M. Pomerantsev, V. M. Ryzhkov, and G. V. Skrotskii, *Physical Principles of Quantum Magnetometry* (Nauka, Moscow, 1972) [in Russian].
2. E. B. Aleksandrov and A. K. Vershovskii, Phys. Usp. **52**, 605 (2009).
3. *Optical Magnetometry,* Ed. by D. Budker and D. F. J. Kimball (Cambridge Univ. Press, New York, 2013).
4. E. B. Aleksandrov, M. V. Balabas, A. K. Vershovskii, et al., Opt. Spectrosc. **78**, 292 (1995).
5. C. Affolderbach, A. Nagel, S. Knappe, et al., Appl. Phys. B **70**, 407 (2000).
6. P. D. D. Schwindt, S. Knappe, V. Shah, et al., Appl. Phys. Lett. **83**, 6409 (2004).
7. S. Groeger, G. Bison, J.-L. Shenker, et al., Eur. Phys. J. D **38**, 239 (2006).
8. V. L. Velichansky, A. N. Kozlov, E. V. Zhivun, et al., Usp. Sovrem. Radioelektron. **12**, 43 (2013).
9. A. Weis, G. Bison, and A. S. Pazgalev, Phys. Rev. A **74**, 033401 (2006).
10. G. D. Domenico, G. Bison, St. Groeger, et al., Phys. Rev. A **74**, 063415 (2006).
11. V. V. Vassiliev, S. A. Zibrov, and V. L. Velichansky, Rev. Sci. Instrum. **77**, 013102 (2006).
12. V. V. Yashchuk, D. Budker, and J. R. Davis, Rev. Sci. Instrum. **71**, 341 (2000).
13. Yu. V. Afanas'ev, N. V. Studentsov, V. N. Khorev, et al., *Measuring Tools of Magnetic-Field Parameters* (Energiya, Leningrad, 1979) [in Russian].
14. A. K. Vershovskii, Doctoral (Phys. Math.) Dissertation (SPb. State Univ., St. Petersburg, 2007).
15. E. B. Aleksandrov, A. S. Pazgalev, and J. L. Rasson, Opt. Spectrosc. **82**, 10 (1997).

Translated by R. Tyapaev